Modelling and Emulation of an Unbalanced LV Feeder with Photovoltaic Inverters

Ramón López-Erauskin
Johan Gyselinck, *IEEE Member*
Bio-, Electro- and Mechanical Systems department
Université Libre de Bruxelles
rlopezer@ulb.ac.be, johan.gyselinck@ulb.ac.be

Frédéric Olivier, *IEEE Student Member*
Damien Ernst, *IEEE Member*
Department of Electrical Engineering and Computer Science
Université de Liège
frederic.olivier@ulg.ac.be, dernst@ulg.ac.be

María Emilia Hervás, Alexis Fabre
GreenWatch SA
Wavre, Belgium
premasol@greenwatch.be

***Abstract*—In this paper, the penetration of grid-connected photovoltaic systems is studied, experimentally tested and compared to simulation results. In particular, how the inverse current flow and unbalance situations affect the voltage in the low-voltage grid. Thus, a test platform has been developed for obtaining experimental results with grid-tied commercial inverters. Photovoltaic arrays are emulated and subjected to different irradiance profiles and the inverters are controlled to produce at different power conditions. A model has been developed in order to reproduce the same operating conditions and working environment. Simulations are performed with the software PowerFactory and the results compared to the experimental ones.**

***Index Terms*—distributed power generation, photovoltaic systems, power distribution, reactive power.**

I. Introduction

The operation of grid-tied photovoltaic (PV) units is characterized by several uncertainties due to the number of currently operating units, the points where they are connected, and the delivered power. Due to the historical design of low-voltage (LV) feeders, PV generation (PVG) can have adverse effects and cause voltage deviations due to reversed power flow [1]. Some authors have also studied the overvoltage in low-voltage grids based in probabilistic models [2], [3]. In this context, a scheme that controls the active and reactive power of inverters was previously designed and numerically tested [4]. The first step toward the validation of the control scheme in a real setting is to reproduce in a laboratory the behavior of a LV feeder under different voltage and unbalance conditions.

In previous research, the impact of the penetration of PV units in the low-voltage network with dispersed loads was investigated [5], [6]. The former presents modeling and field measurements and addresses the problems of increasing PV installations in these networks. In the latter, a benchmark LV microgrid network is presented, which is suitable for steady state and transient simulations. In validation, laboratory reproduction allows time-, cost- effective and repeatable tests of overvoltage conditions of the grid without need of deploying expensive equipment close to large concentrations of PV systems.

In this paper, we present the test platform (Fig. 1) emulating a LV feeder, and the voltage and power variations for several operation scenarios. The effect of active and reactive power variations on the voltage profile is studied. The lab feeder is modeled numerically and simulations are performed for each operation scenarios. The results from the measurements and the simulations are then compared.

II. Test platform and model in PowerFactory

A LV feeder is composed of several elements: the main ones are the external grid, the distribution transformer, the cables, the PV systems and the loads which represent houses consumptions. In our study, loads are not considered. Since they would be connected at the same point as the PV systems, they would reduce the power injected into the network and thus decrease the voltage variations, a behavior that we specifically want to exhibit in our simulations. In this section, every part of the test platform in Fig. 1 is described and its lab implementation explained. The network reproduced in the lab is modeled in PowerFactory, a power system analysis software, with the electrical and hardware characteristics of the external grid, cables and inverters to allow a meaningful comparison.

A. External grid

In a typical setting, the external grid would be the medium voltage network at a voltage close to 15 kV and the distribution transformer would bring this voltage down to 400 V. In the lab setting, the external grid is the low voltage network. In PowerFactory, it is modeled as a slack bus with a constant voltage.

B. Distribution transformer

The transformer that feeds the reproduced LV-grid has the following characteristics: Δ-Y configuration, $S_{trafo} = 100$

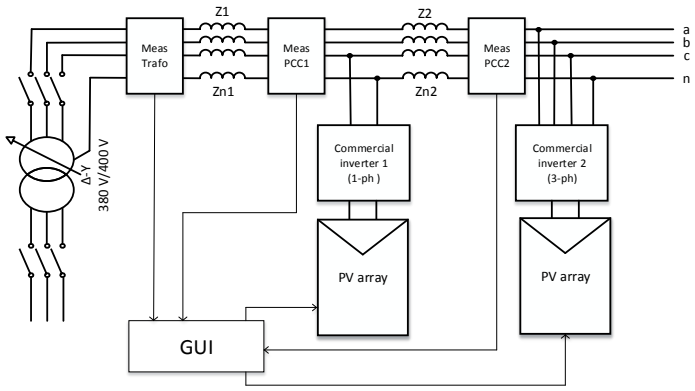

Fig. 1. Laboratory test bench for the study of voltage fluctuations and unbalanced conditions

kVA, the Primary (380 V, three-phase, delta) and the Secondary (400 V, three-phase, four-wire). In particular, abnormal grid conditions can be emulated with e.g. undervoltage or overvoltage in order to test the behaviour and the compensation features of the inverters. The impedance is estimated considering the standardized short-circuit voltage for distribution transformers (where $\omega = 2 \cdot \pi \cdot f$ is the angular frequency and f = 50 Hz) [10], as follows:

$$V_{CC} = 4\% \; V_{ph-n} = 0.04 \cdot 230V = 9.2V \tag{1}$$

Where the short-circuit current is

$$I_{CC} = \frac{S_{trafo}}{\sqrt{3} \; V_{Nom}} = \frac{100kVA}{\sqrt{3} \; 400} = 144A, \tag{2}$$

and the value of the reactance and inductance is calculated:

$$X_{L,trafo} = \frac{V_{CC}}{I_{CC}} = 64m\Omega \tag{3}$$

$$L_{trafo} = \frac{X_{L,trafo}}{\omega} = 204\mu H \tag{4}$$

In PowerFactory, the transformer is modeled considering its short-circuit voltage, copper losses, iron losses and magnetizing impedance.

C. Cables

The impedance characteristics of the feeder are important as they will determine the actual voltage variations inside the feeder (see section III). The cables are reproduced in the test bench placing impedances between the transformer and the points of connections of the inverters (PCC) as in Fig. 1. The values of the impedances are gathered in Table I.

D. PV systems

1) PV array emulator: The PV array emulator allows the reproduction of the characteristics of a standard PV installation in a flexible manner [7]. It uses the single-exponential model of the solar cells [8] with an adjustable number of panels in parallel and series in function of the output characteristics required and takes into account the influence of the in-plane irradiance and the PV cell temperature. The characteristic parameters of the PV panels used for the PV array emulation are grouped in Table II. The emulator is able to reproduce realistic atmospheric conditions either with the clear-sky model or actual recorded data. In addition, shading can be easily set in the Graphical User Interface (GUI) of the emulator in order to test the Maximum Power Point Tracking (MPPT) capabilities of the PV inverters under these conditions [7], [9]. In particular, shading results in several local maxima on the instantaneous Power-Voltage (P-V) curve of the PV array, which requires an appropriate algorithm for proper MPPT.

TABLE I
CABLE PARAMETERS

Symbol	Description	Value	Units
R	Phase line resistance	0.1	Ω
X	Phase line reactance	65.97	mΩ
R_N	Neutral line resistance	0.165	Ω
X_N	Neutral line reactance	370.7	mΩ

TABLE II
PARAMETERS OF ONE PV PANEL

Symbol	Description	Value	Units
V_{OC}	Open-circuit voltage	37.3	V
I_{SC}	Short-circuit current	8.52	V
V_{MPP}	MPP voltage	30.5	V
I_{MPP}	MPP current	8.04	V
P_{MPP}	MPP power	245.22	W

TABLE III
CONFIGURATION OF THE PV ARRAYS

Array	N. of panels	Vmax (V)	Peak power (W)
Array 1	11	410.3	2697.42
Array 2	20	746	4904.4

2) Commercial inverter: The inverter, through which the PV array is connected to the LV grid, is commonly designed to comply with the latest grid standards. For this reason, compensation features to help support the grid are more and more often implemented by the manufacturers. In commercial inverters, this includes mainly power regulation through active power reduction (w.r.t. the default maximum power production) and reactive power compensation. The former is introduced in order to limit the power delivered for a specific section of the grid and the latter to correct locally some power quality issues such as voltage fluctuations.
Depending on the inverter, the reactive power compensation

can be set in different ways; it can be adapted to the needs of the system (so-called static or dynamic cosφ setpoint) or to the country grid codes. For example, the German grid codes require the reactive power setpoint to be either fixed or adjustable by a signal from the network operator. The setpoint value is either a fixed displacement factor (static cosφ), a variable displacement factor depending on the active power ($\cos\varphi(P)$), a fixed reactive power value in VAr (dynamic cosφ) or a variable reactive power depending on the voltage $Q(U)$ [11]. These features have been previously tested and the voltage compensation capabilities of the inverters assessed [12]. In order to adjust the power setpoints, it is necessary to allow the communication between the user (e.g. network operator) and the inverter. This is done using the RS485 communication protocol, setting absolute values of the active and reactive powers or the cosφ parameter.

TABLE IV
PARAMETERS OF THE SINGLE-PHASE INVERTER

Symbol	Description	Value	Units
V_{DC-MPP}	DC-voltage MPPT range	350 - 600	V
P_{DC-Max}	Maximum DC input power	3200	W
V_{AC}	AC rms voltage (ph-N)	230	V
P_{AC}	Nominal AC power	2600	VA
$\cos\varphi$	Power factor	-0.8..1..0.8	-

TABLE V
PARAMETERS OF THE THREE-PHASE INVERTER

Symbol	Description	Value	Units
V_{DC-MPP}	DC-voltage MPPT range	245 - 800	V
P_{DC-Max}	Maximum DC input power	5150	W
V_{AC}	AC rms voltage (ph-ph)	400	V
P_{AC}	Nominal AC power	5000	VA
$\cos\varphi$	Power factor	-0.8..1..0.8	-

The characteristics such as the configuration of the PV arrays and the peak power for the single- and three-phase inverters are specified in Table III, IV and V.

E. The Graphical User Interface

ControlDesk software is used together with the dSPACE ds1104 platform for the GUI. The user can observe the relevant system variables, such as the grid voltages and currents, and the DC-side voltage and current. Also, the instantaneous characteristic curves of the PV array for the adjustable meteorological conditions set are displayed, so that the evolution of the working point can be observed. This is especially useful for evaluating the MPPT capability of the inverter.

III. VOLTAGE FLUCTUATION

The validation of the results obtained in the simulation are of relevant importance in order to ensure the reliability of a simulation model. For that purpose, the power exchange between the PVGs and the LV feeder will be tested here to see how it affects to the grid voltage. The relation between power exchange and voltage fluctuation is discussed hereafter [13].

As shown in Fig. 1, any current flow will generate a voltage drop and a phase shift between two arbitrary points on the feeder. In LV feeders, to which distributed generation units are commonly connected, the inductive and resistive components have to be considered [13]. Considering no load connected at any PCC, the complex power flowing through that section is the one coming from the PV inverters: $S_{inv} = P_{inv} + jQ_{inv}$. The voltage at the PCC1 is here considered as reference with $V_1 = V_1\angle 0°$ while the one at the transformer $V_{tr} = V_{tr}\angle\delta$ and the grid current $I = I\angle\varphi$ are phase-shifted by angles δ and φ, respectively. The complex power at the PCC1 is, therefore, the sum of the powers delivered by the inverters and expressed as $S_{PCC-1} = P_{PCC-1} + jQ_{PCC-1}$.

In unbalanced condition for this LV feeder configuration, the existing neutral impedance displaces the neutral voltage V_{N1} from the one at the transformer (V_N). Represented in Fig. 2, V_A, V_B and V_C (in dark blue) are the line voltages at PCC1. The single-phase inverter is connected between phase C and the neutral point, where the inverter voltage is in phase with V_C (Fig. 3).

The voltage drop at the impedance between the transformer and the PCC1 is:

$$\underline{\Delta V}_1 = \underline{Z}_1 \cdot \underline{I} \tag{5}$$

considering the feeder impedance $\underline{Z}_1 = R_1 + jX_1$. The phase A voltage at the transformer is, therefore:

$$\underline{V}_{AN} = \underline{V}_A - \underline{\Delta V}_1 \tag{6}$$

and its neutral point voltage:

$$\underline{V}_N = \underline{V}_{N1} + \underline{\Delta V}_{LN} \tag{7}$$

where $\underline{V}_{N1}$ is the neutral voltage at PCC1 and $\underline{\Delta V}_{LN}$ is the voltage drop at the neutral impedance Z_{N1}, caused by the current $\underline{I}_N$ flowing through the neutral line:

$$\underline{\Delta V}_{LN} = \underline{I}_N \cdot \underline{Z}_{N1} \tag{8}$$

considering the neutral impedance $\underline{Z}_{N1} = R_{N1} + jX_{N1}$. The neutral voltage at PCC-1 satisfies the following expression:

$$\underline{V}_{N1} = \underline{V}_N - \underline{\Delta V}_{LN} \tag{9}$$

and the phase A to neutral voltage at PCC-1 is:

$$\underline{V}_{AN1} = \underline{V}_A - \underline{V}_{N1} \tag{10}$$

The displacement of $\underline{V}_{N1}$ from the neutral point of the transformer $\underline{V}_N$ causes a decrease in the magnitude of the vector in phase A and the resulting effect on the voltages (in light blue) at PCC1.

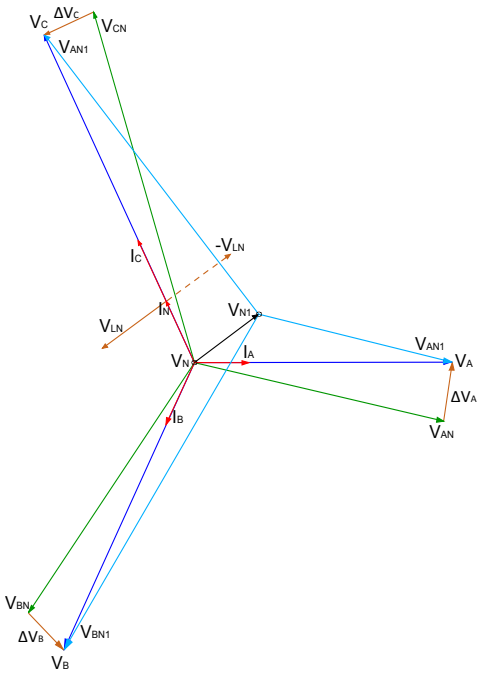

Fig. 2. Voltage phasors of the LV feeder at PCC-1

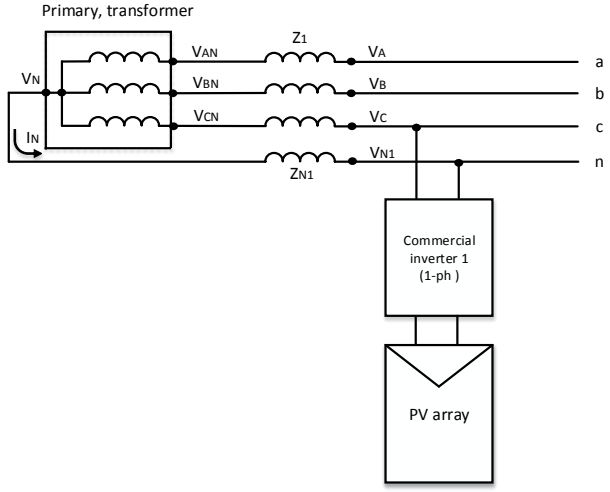

Fig. 3. Part of the laboratory test platform and the neutral current flow direction

IV. Results and Comparison

The testing is done for single- and three-phase inverters, focusing on their power regulation functionality and the resulting voltage compensation capability. The general parameters of the platform are shown in Table I.

The simulations are performed in two different phases:

A. Static production values

The different operating scenarios are:

1) Operating scenario 1 (OP1): all PV inverters produces their maximum active power.
2) Operating scenario 2 (OP2): all PV inverters produce half their maximum power.
3) Operating scenario 3 (OP3): all PV inverters produce half their maximum active power and absorb the maximum reactive power. This last operating scenario allows us to observe the influence of reactive power on the voltages at the LV level.

TABLE VI
Active and Reactive Power Produced by the Inverters in Each Scenario

	Single-phase inverter		Three-phase inverter	
	P (W)	Q (var)	P (W)	Q (var)
OP1	2317	0	4810	0
OP2	1200	0	2460	0
OP3	1200	-1700	2460	-2500

The three OPs show the voltage fluctuation in a LV feeder in presence of dispersed generation, where the consumption is null. The goal of these simulations is to put in evidence the phenomenon by which a overvoltage can occur. In that regard, power consumption was not considered as it would reduce the power injected in the different PCCs and diminish the effect of power on voltage.

Figs. 4-6 show the voltage profile evolution for simulation (dashed lines) and experimental (solid lines) results for the different scenarios and the impact of PVG and reactive power on voltage.

1) OP1: In Fig. 4, all the inverters are producing at their maximum power, without reactive power compensation. The figure shows the influence of the injected power on the grid voltage for each PCC. The furthest the PVG is from the LV feeder transformer, the highest is the voltage level at the PCC for V_{bn} and V_{cn}. In this situation, the generators linked to it are the first to disconnect from the grid if an overvoltage occurs. However, the same does not apply to V_{an}, affected by the displacement of the neutral voltage V_{N1} from the neutral point of the transformer V_N, as explained in section III.

2) OP2: In Fig. 5 the inverters are working at half their maximum active power with a lower influence in the voltage increment.

3) OP3: For this scenario, the voltage at phase C decreases more notably than at the others due to the two inverters' reactive power consumption.

According to (5)-(10), the voltage drop (ΔV) at the line impedance depends on the feeder characteristics, the direction of the current and the amount of this current. The behavior of the voltage profile along the different points of the feeder is, in most of the cases, the same for both simulation and experimental results. The differences between the numerical

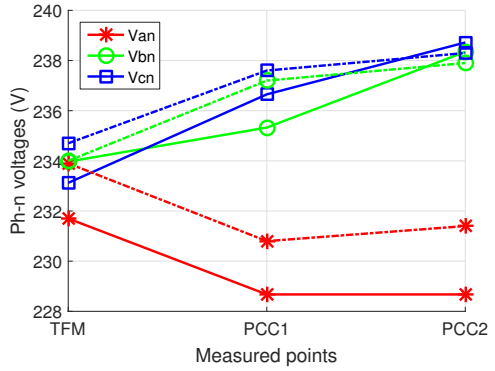

Fig. 4. Voltage profile of the LV feeder, PV inverters producing at full power. Simulation (dashed lines) and experimental (solid lines) results.

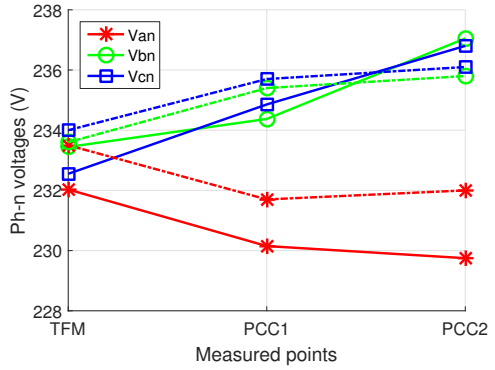

Fig. 5. Voltage profile of the LV feeder, PV inverters producing at half maximum power. Simulation (dashed lines) and experimental (solid lines) results.

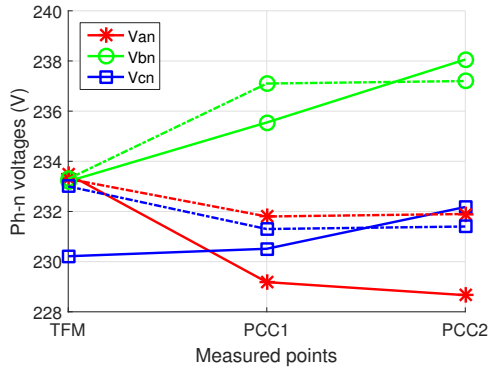

Fig. 6. Voltage profile of the LV feeder, PV inverters producing at half maximum power and absorbing maximum reactive power. Simulation (dashed lines) and experimental (solid lines) results.

results and the measured ones (e.g. measured V_{an} = 231.7 V and simulated V_{an} = 233.9 V in Fig. 4) are due to the voltage differences in the real transformer, not reproducible in software reliably. However, these divergences need to be studied more deeply to bring the simulations and the real environment measurements closer.

Table VII gathers the values of Figs. 4-6 for the three different operation scenarios: OP1, OP2, and OP3, where the added letter "L" means "Laboratory" and "S" "Simulation".

TABLE VII
VOLTAGES MEASURED AT THE LV FEEDER

Operation scenario	OP1L	OP1S	OP2L	OP2S	OP3L	OP3S
$V_{an,Tr}$ (V)	231.7	233.9	232	233.5	233.5	233.3
$V_{bn,Tr}$ (V)	233.9	234	233.4	233.6	233.2	233.3
$V_{cn,Tr}$ (V)	233.1	234.7	232.5	234	230.2	233
$V_{an,PCC1}$ (V)	228.7	230.8	230	231.7	229	231.8
$V_{bn,PCC1}$ (V)	235.3	237.2	234.4	235.4	235.5	237.1
$V_{cn,PCC1}$ (V)	236.7	237.6	234.9	235.7	230.5	231.3
$V_{an,PCC2}$ (V)	228.7	231	229.8	232	228.7	231.8
$V_{bn,PCC2}$ (V)	238.4	237.9	237	235.8	238.1	237.2
$V_{cn,PCC2}$ (V)	238.7	238.3	236.8	236.1	232.2	231.4

B. Dynamic production values

The PV array emulators follow predefined irradiance profiles to simulate realistic behavior of the inverters during a day. The irradiance profile used for the simulations is the one of a sunny day in Belgium and its acquisition time is 1 minute. The variation of the irradiance is reproduced in the laboratory every 2 seconds, accelerating the execution 30 times. This way, faster experimental results than in field measurements can be obtained, as can be seen in Fig. 8. The variation of voltages, active and reactive power flows are studied and compared to the numerical results to validate them thanks to the real hardware emulation.

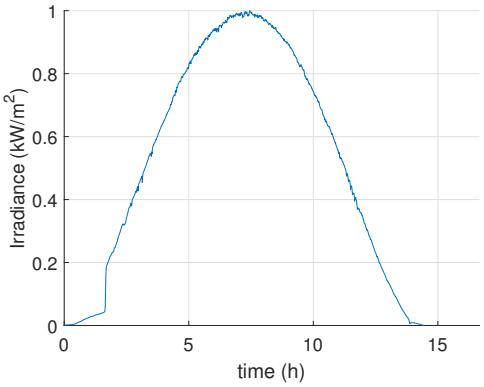

Fig. 7. Irradiation profile during a sunny day

Fig. 9 shows the evolution of the output voltages of the inverters, as well as the active and reactive power flows that corresponds to the irradiance profile for a sunny day (Fig. 7). The output behavior of the inverters is analyzed in the PowerFactory model, as for the static production values, with the same predefined parameters as in the test platform. The results obtained also present a similar evolution, although the voltage differences between phases cannot be reproduced with PowerFactory due to an small initial unbalance in the test platform.

V. CONCLUSIONS

In this manuscript, an unbalanced LV feeder caused by the grid-tied inverters has been studied for different values

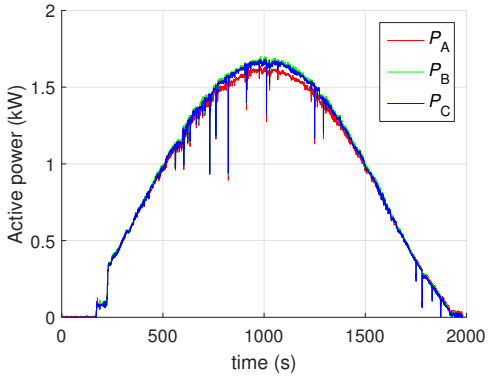

Fig. 8. Time variation of the active power at PCC2 during a sunny day

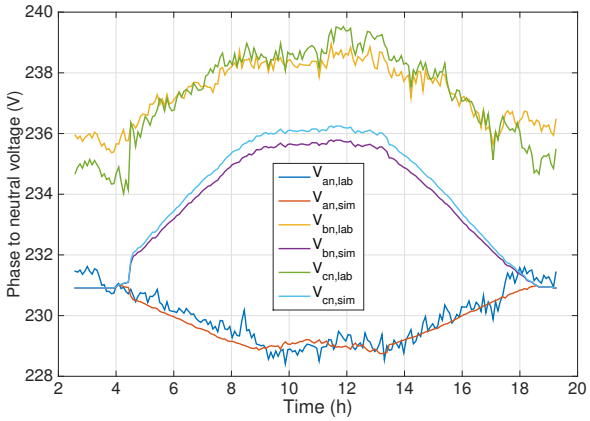

Fig. 9. Time variation of the phase-to-neutral voltages at PCC2 during a sunny day

of active and reactive power production. A test bench that reproduces an specific LV feeder has been designed for this study and its behavior compared to its numerical model. This comparison has illustrated the reproduction of a similar behavior between the experimental work and the simulated model but also the difficulties of obtaining reliable results in simulations, due to the lack of information for some of the parameters of the system. In addition, the effect of local neutral point displacement has been exhibited and explained. It changes the shape of the phase-to-neutral voltages in magnitude and phase and can aggravate the unbalance situation.

ACKNOWLEDGEMENT

This research is financed by the Walloon region in the framework of the PREMASOL project (C-6829).

REFERENCES

[1] P. P. Barker and R. W. De Mello, "Determining the impact of distributed generation on power systems. I. Radial distribution systems," *Power Eng. Soc. Summer Meet*, vol. 3, pp. 1645-1656, 2000.

[2] V. Klonari, F. Vallee, O. Durieux, J. Lobry, "Probabilistic tool based on smart meters data to evaluate the impact of distributed photovoltaic generation on voltage profiles in low voltage grids," *Solar Integraton Workshop*, 2013.

[3] V. Klonari, F. Vallee, O. Durieux, Z. De Greve, J. Lobry, "Probabilistic Modeling of Short Term Fluctuations of Photovoltaic Power Injection for the Evaluation of Overvoltage Risk in Low Voltage Grids," *IEEE International Energy Conference (ENERGYCON).*, pp. 897-903, 2014.

[4] F. Olivier, P. Aristidou, D. Ernst, and T. Van Cutsem, "Active Management of Low-Voltage Networks for Mitigating Overvoltages Due to Photovoltaic Units," *IEEE Trans. Smart Grid*, pp. 1-9, 2015.

[5] Ioulia T. Papaioannou, Minas C. Alexiadis, Charis S. Demoulias, Dimitris P. Labridis, and Petros S. Dokopoulos, "Modeling and Field Measurements of Photovoltaic Units Connected to LV Grid. Study of Penetration Scenarios," *IEEE Trans. Power Delivery*, vol. 26, no. 2, pp. 979-987, April 2011.

[6] S. Papathanassiou, N. Hatziargyriou, K. Strunz "A Benchmark Low Voltage Microgrid Network," *CIGRE Symposium*, 2005.

[7] T. Geury, and J. Gyselinck, "Emulation of photovoltaic arrays with shading effect for testing of grid- connected inverters," *Proc. 2013 EPE European Conference on Power Electronics and Applications.*, pp. 1-9.

[8] M. G. Villalva, J. R. Gazoli, and E. R. Filho, "Comprehensive approach to modeling and simulation of photovoltaic arrays," *IEEE Trans. Power Electron.*, vol. 24, no. 5, pp. 11981208, May 2009.

[9] I. R. Balasubramanian, S. Ilango Ganesan, and N. Chilakapati, "Impact of partial shading on the output power of pv systems under partial shading conditions," *IET Power Electron.*, vol. 7, no. 3, pp. 657666, 2014.

[10] B. Metz-Noblat, F. Dumas, and C. Poulain, "Calculation of short-circuit currents," Scheinder Electric, Grenoble, France, Tech. Rep. TR-0158, p. 13, 2005.

[11] E. Troester, "New german grid codes for connecting pv systems to the medium voltage power grid," *2nd Int. Work. Conc. Photovolt. Power Plants Opt. Des. Prod. Grid Connect.*, pp. 1-4, 2009.

[12] R. Lopez-Erauskin, T. Geury, A. Gonzalez, J. Gyselinck, M.E. Hervas, A. Fabre, "Testing the Enhanced Functionalities of Commercial PV Inverters Under Realistic Atmospheric and Abnormal Grid Conditions ," *Solar Integraton Workshop*, 2015.

[13] R. A. Mastromauro, M. Liserre, and A. D. Aquila, "Single-phase grid-connected photovoltaic systems with power quality conditioner functionality," *European Conference on Power Electronics and Applications*, pp. 1-11, 2007.

[14] R. Kabiri, D. G. Holmes, and B. P. McGrath, "The influence of pv inverter reactive power injection on grid voltage regulation," *IEEE 5th Int. Symp. Power Electron. Distrib. Gener. Syst.*, pp. 1-8, Jun. 2014.